Microstructural Modifications in an Explosively Welded Ti/Ti Clad Material: I. Bonding Interface

M. NISHIDA, A. CHIBA, K. IMAMURA, H. MINATO, and J. SHUDO

Microstructural modifications of the bonding interface in an explosively welded Ti/Ti clad material using the preset angle standoff configuration with various flyer plate speeds have been studied. Explosive welding was completed at flyer plate speed over 420 m/s. The wavelength and amplitude of the wavy interface increased with increasing flyer plate speed up to 1060 m/s. The planar interface was obtained at flyer plate speed of 1150 m/s. The trace of melting was observed at the bonding interface in the present experimental conditions. It is concluded that the melting layer is responsible for the bonding of explosively welded Ti/Ti clad materials. An anomaly hardening zone was formed at the bonding interface in the clad material welded at flyer plate speed of 1150 m/s. The origin of the observed anomalous hardening has also been discussed.

I. INTRODUCTION

THE application of clad materials has been widely spread in various engineering fields and industries, such as chemical, petroleum, power plant, and shipbuilding industries.[1] Among clad materials, the cladding of titanium to other metals and alloys has been drawing particular interest in the connection with corrosion and heat resistance of the titanium. The industrially used cladding processes are hot-rolling, diffusion bonding, overlay welding, enshrouding casting, and explosive welding, as have been reviewed by Kawanami.[1] Any one of these processes has both advantages and disadvantages. One of the positive aspects of explosive welding is the capability of formation of an intimate contact between two materials that cannot be bonded with conventional methods.[2,3]

The principle of explosive welding is briefly summarized as follows.[2,3] The top (flyer) plate is set parallel (constant standoff) or obliquely to the bottom (parent) one with appropriate standoff distance. The latter configuration is the preset standoff angle configuration, which was used in the present study, as illustrated in Figure 1. Explosives are put on the upper surface of the flyer plate. As the explosive is initiated with the electrical detonator, the flyer plate is drastically accelerated by the detonation pressure and flies with high speed toward the parent plate. The standoff provides the distance across which the flyer plate can be accelerated at the necessary impact velocity. This is the most important reason for the initial standoff. Since this flight occurs with the progress of the detonation wave from the priming side to the opposite one, the dynamic bend angle is related to the flight and the detonation speed. Subsequently, the flyer plate collides with the bottom plate, and then a jet of metal is formed at the apex of the collision, which removes the oxide layer and other impurities on both surfaces to be welded. The standoff also provides an unobstructed exit path for the free jet and air between the plates. This is the second reason for the initial standoff. At the collision point, fresh metal surfaces enter with high impact into intimate contact and metallurgical bonding is completed along the interface within a few microseconds. Therefore, explosive welding is useful in the joining of such active metals as titanium, which is easily oxidized. It is well known that the bonding interface has a wavy shape in explosive welding. The characteristics of the shape for a given set of materials being welded depend on such cladding parameters as detonation speed and mass of explosive, geometry of assembly, *etc.*[2–7] It is evidently expectable that a variety of microstructural modifications are induced in and around the bonding interface by severe deformation and thermomechanical processes. A detailed microstructural analysis of the bonding region by transmission electron microscopy (TEM) is a useful technique to obtain a better understanding of the phenomena associated with explosive welding and of the bonding mechanism. So far, few investigations have been made in this field,[3–7] while the residual microstructural modifications developed in shock-loaded materials[8–18] have been more extensively studied than those in explosively welded materials in spite of their similarity.

The purpose of the present study is to clarify the bonding mechanism and the microstructural modifications of the bonding interface in an explosively welded Ti/Ti clad material for basic research of the explosive cladding of titanium to other metals and alloys. It is also interesting to study the residual microstructures of shock-loaded materials, because titanium is a target material and is known to form the characteristic shock-induced microstructures that are typically represented by adiabatic shear bands (ASBs).[9–12] The latter part will be described in the companion article.[19]

II. EXPERIMENTAL PROCEDURE

A commercially pure grade of titanium (TP-35H, provided by Nippon Steel Corporation, Hikari 743, Japan),

M. NISHIDA, Associate Professor, A. CHIBA, Professor, and K. IMAMURA, Technician, are with the Department of Materials Science and Resource Engineering, Faculty of Engineering, Kumamoto University, Kumamoto 860, Japan. H. MINATO and J. SHUDO, formerly Graduate Students, Department of Materials Science and Resource Engineering, Kumamoto University, are Research Engineers, the Nippon Steel Corporation, Kitakyushu 805, Japan, and Daido Special Steel Corporation, Nagoya 476, Japan, respectively.

Manuscript submitted April 22, 1992.

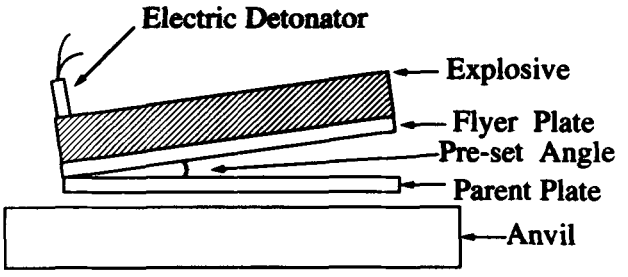

Fig. 1—Schematic illustration of experimental assembly for explosive welding.

indicated in Table I, was used in this study. Before cladding, plates of titanium 90 × 40 × 5 mm^3 in size were annealed at 1073 K for 100 hours in a vacuum of 2 × 10^{-3} Pa and subsequently furnace-cooled to produce a coarse-grained structure. They were mechanically ground to remove the oxide scale, polished with emery paper, and finally rinsed in acetone with ultrasonic cleaner. Figure 2 shows optical micrographs of the resultant microstructure. The α-equiaxed grains are seen, and their average grain size is about 700 μm in diameter. No microstructural feature, other than grain boundaries and a few dislocations, was observed on a TEM scale. A preset angle standoff configuration was used for the present explosive welding experiment, as mentioned previously. The preset angle was 7 deg. Plastic explosive (SEP, provided by Asahi Chemical Industry Co., Ltd., Chiyoda, Tokyo 100, Japan) consists mainly of nitric ester. The detonation velocity of the explosive was about 6900 m/s. The explosive cladding parameters are listed in Table II. The flyer plate velocities were varied from 320 to 1150 m/s in average and were measured with pin-contact technique[20] at the plateau region of wavelength and amplitude in wavy interface, as described subsequently. The collision pressure P was estimated using the following equation:[21]

$$P = 1/2\rho V_p V_s$$

where ρ is density of titanium, V_p is flyer plate velocity, and V_s is sound velocity in titanium. The collision pressures are calculated to be from 3.5 to 12.7 GPa, as listed in Table II. After explosive welding, specimens for optical microscopy were cut parallel to the detonation direction from the various positions, electropolished in an electrolyte consisting of 6 pct perchloric acid and 94 pct acetic anhydride in volume, and etched in a solution consisting of 1 pct hydrofluoric acid, 1.5 pct hydrochloric acid, 2.5 pct nitric acid, and 95 pct distilled water in volume. The specimens were used for measurements of the wavelength and amplitude of the wavy interface. The plateau of the wavelength and amplitude was observed at about 15 to 70 mm from the priming point. Therefore, the specimens used in the following experiments were collected from this region. Vickers microhardness tests were also carried out in and around the bonding interface. Specimens for TEM observations were prepared from slices that were cut parallel to the detonation direction and mechanically ground to a thickness of about 0.2 mm. Disks of 3 mm in diameter, containing the bonding interface, were punched out and electropolished using the twin-jet method in an electrolyte consisting of 5 pct perchloric acid, 35 pct n-butyl alcohol, and 60 pct methanol in volume. Electron diffraction and TEM observations were carried out in a JEOL 2000-FX microscope operated at 200 kV and equipped with a ± 45 deg double tilt holder.

Auger electron spectroscopy (AES) was used to establish the distribution of impurity elements across the bonding interface. Analysis was performed in a JEOL JAMP-30 auger microprobe.

Table I. Chemical Composition of Ti Plate (Mass Percent)

C	H	O	N	Fe	Ti
0.01	0.001	0.15	0.01	0.04	balance

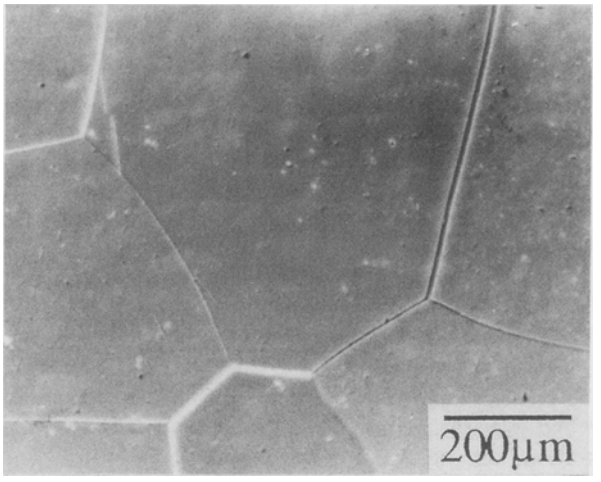

Fig. 2—Optical micrograph showing a coarse-grained structure of the original Ti plate.

Table II. Cladding Parameters in Experiments

System	Flyer Plate Speed (m/s)	Collision Pressure (GPa)
I	320	3.5
II	420	4.6
III	590	6.4
IV	820	8.9
V	1060	11.6
VI	1150	12.7

III. RESULTS AND DISCUSSION

A. *Macroscopic Features in and around the Bonding Interface*

Explosive welding was complete in systems II to VI at flyer plate speed of over 420 m/s, as listed in Table II. Figure 3 shows the relation between average wavelength and amplitude of the wavy interface in the plateau region mentioned in Section II and flyer plate

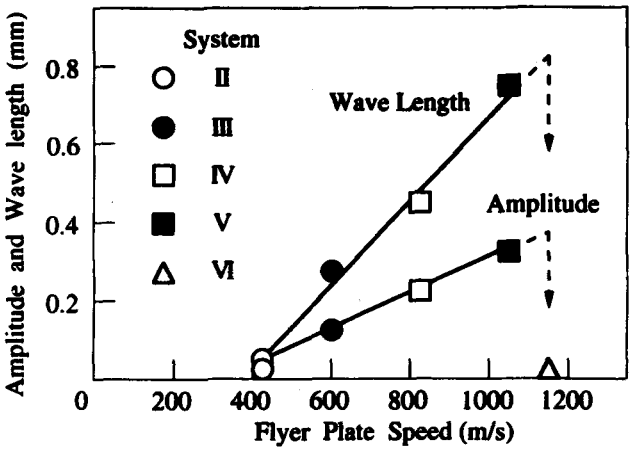

Fig. 3—Variations of average wavelength and amplitude of the wavy interface with flyer plate speed.

speed in the welded materials. The wavelength and amplitude increase linearly with increasing flyer plate speed up to 1060 m/s. However, both values are nearly zero in system VI at a flyer plate speed of 1150 m/s. That is, planar interfaces were formed in system VI. The morphology of bonding interface in systems II, IV, and VI is shown in Figure 4, where larger arrows show the detonation direction. For convenience, the detonation direction of each micrograph is standardized in the same direction. Therefore, the parent plate is the bottom side in Figures 4(a) and (b) and the upper side in (c). These features are consistent with the results of Figure 3 in respect to the wavelength and amplitude. The macroscopic features in and around the bonding interface are summarized as follows. The width of bonding interface increases with increasing flyer plate speed, and a melt layer is clearly evident in systems III to VI. Highly dense deformation twins are induced in all systems. Adiabatic shear bands, as indicated by smaller arrows, are observed opposite to the detonation direction in systems IV and VI. That is, ASBs are formed in the clad materials welded at flyer plate speed of more than 820 m/s in the present experiment. In addition, the fine-grained band, similar to the ASB, exists at the bonding interface of the parent plate side in the system VI, as shown by the double arrows in Figure 4(c). This may be related to the formation of a planar interface and will be discussed in Section C. In order to study the effect of flyer plate speed (*i.e.*, collision pressure) on the microstructural modifications in and around the bonding interface, combined use of optical microscopy and TEM has been performed in systems II, IV, and VI.

B. *Microscopic Features of the Bonding Interface*

The size of the bond zone in system II was about 2 μm in width, as shown in Figure 5(a). Deformation structures (*i.e.*, deformation twins and dislocations) can be seen in crystal grains at both sides of the bonding interface. Characterization of these lattice defects will be described in the following article. The bond zone consists of fine grains, which are elongated to the collision direction, having an average grain size of 100 and 250

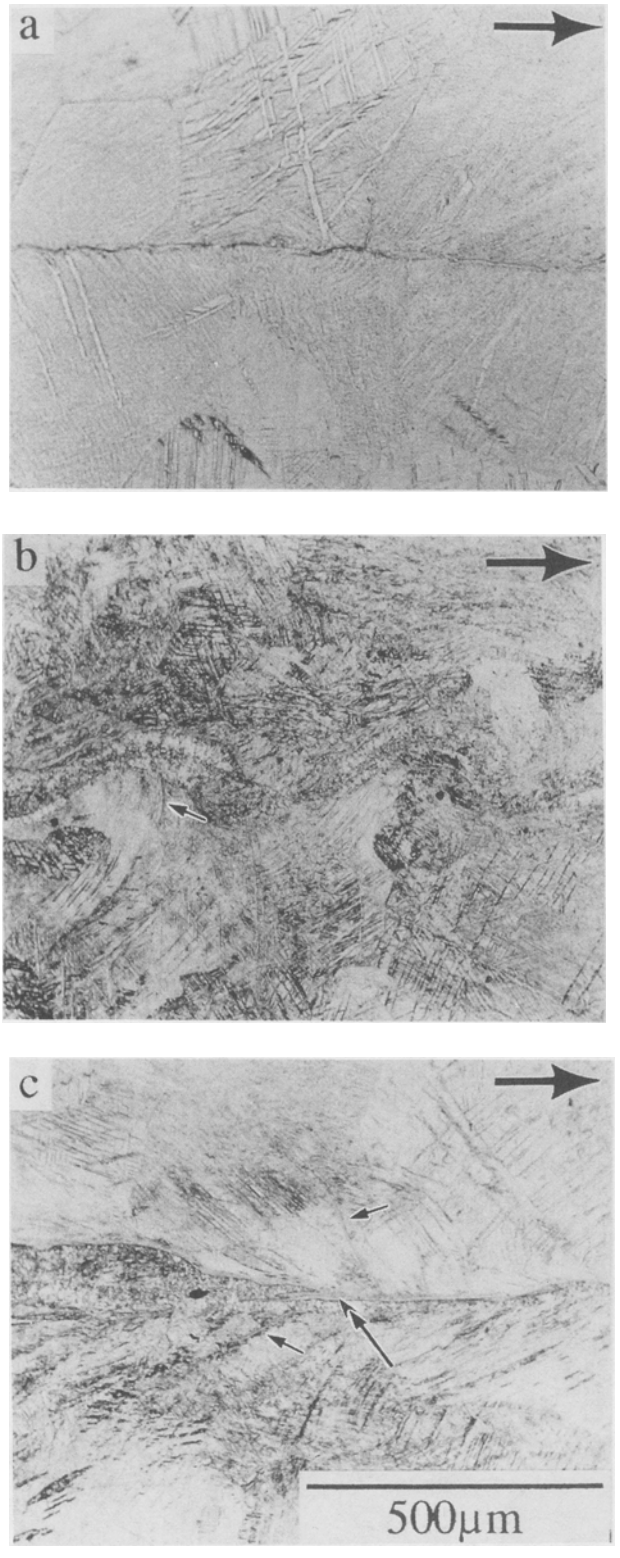

Fig. 4—Optical micrographs of bonding interface in systems (*a*) II, (*b*) IV, and (*c*) VI. Larger, smaller, and double arrows show detonation direction, ASB, and hardening zone described below, respectively. The parent plate is the bottom side in (a) and (b) and the upper side in (c).

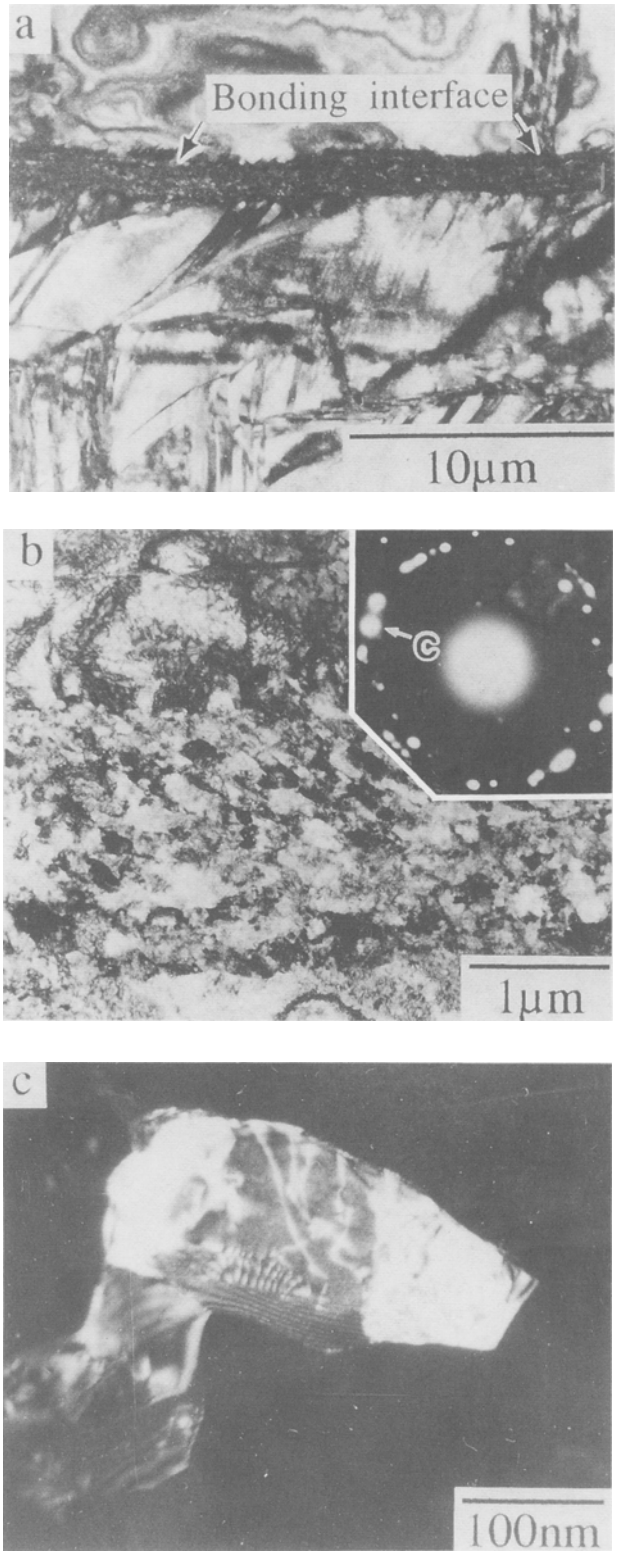

Fig. 5—Transmission electron micrographs of the bonding interface in system II. (*a*) low-magnification and (*b*) enlarged bright-field images and (*c*) a dark-field image taken by using a diffraction spot marked C in the SAD pattern of (a).

nm in width and longitudinal direction, respectively, as shown in Figures 5(b) and (c). These elongated fine grains are randomly oriented, as seen in the inserted electron diffraction pattern in (b). There are a number of dislocation images in the grain interior, as shown in Figure 5(c). The existence of randomly oriented fine grains may indicate the result of the rapid solidification of a thin molten layer formed during the cladding. On the other hand, the elongation of fine grains and the existence of dislocations suggest that a kind of cold pressure welding takes place at bonding interface of system II. It is difficult to define the bonding mechanism in system II. However, a thin, amorphous layer, about 0.1 to 1.0 μm in width, was observed at the bonding interface in Ti/SUS 304 and 430 stainless steel clad materials.[22] This was a resultant product of rapid solidification after melting of the bonding interface during explosive welding. Consequently, the presence of bond zone[5] is evident and may be related to the melting of bonding interface.

Figure 6 shows enlarged optical micrographs of the bonding interface in system IV, which consists of grains irregular in size. A transition from columnar to equiaxed grains is observed from the outer region to the center, which is a typical microstructural feature for the solidification of metals and alloys. From these results, the occurrence of melting at bonding interface in system IV is unequivocally confirmed. Figure 7(a) shows a dominant microstructure of the melt zone in system IV. There are some dislocation images in the solidified grains that must have been formed by thermal contraction during cooling. Burgers vector determination of these has not been completed, but many of the dislocations appeared to be **a** or **c** + **a** type, since they were in contrast with both the 0002 and 0110 reflections operating. In the outer region of molten layer, twin lamellae were occasionally observed, as shown in Figure 7(b). The twinning plane of these is determined to be $(1\bar{1}01)$, as can be seen from the electron-diffraction pattern in Figure 7(c). The $\{10\bar{1}1\}$ twinning has been reported as an internal defect of the martensitic phase in quenched pure titanium.[23] It is apparent that martensitic transformation takes place in the

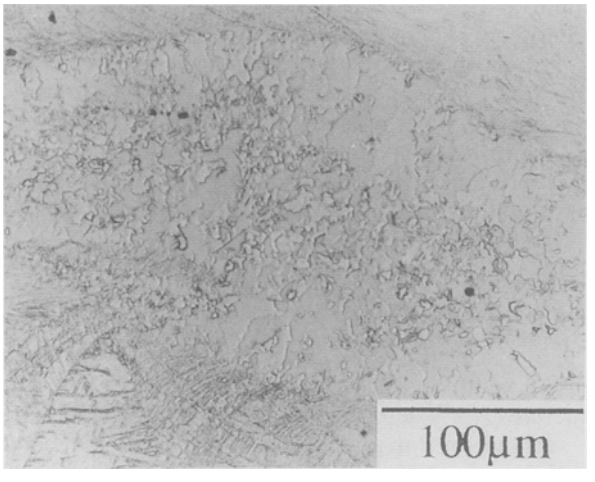

Fig. 6—Optical micrograph of melting zone at the bonding interface in system IV.

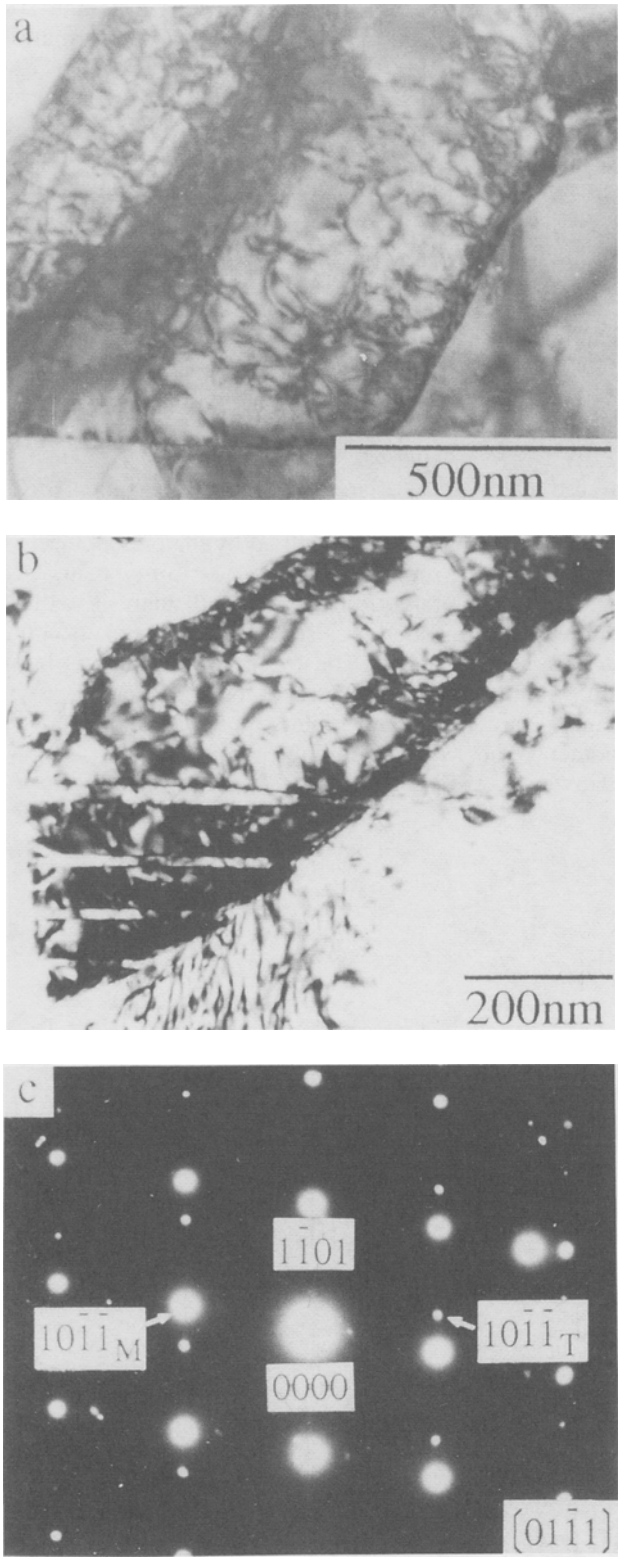

Fig. 7—Transmission electron micrographs of melting zone at the (*a*) center and (*b*) outer region of the bonding interface in system IV and (*c*) corresponding electron diffraction pattern of (b) showing $(1\bar{1}01)$ twinning.

melt zone. It is well known that the self-annealing effect occurs in titanium because of lower quench hardenability due to high transformation temperature and low thermal conductivity. Therefore, the martensitic phase was partially observed in the melt zone, especially at the outer region. It has been reported that equiaxial ultrafine grains, about 0.3 μm in diameter, formed in the melt layer of the bonding interface in explosively welded copper[5,7] and aluminum[6] alloys. However, rather large grains form in the melt zone of the present system. This may also be attributable to the low thermal conductivity of titanium. It has been reported that elongated grains aligned parallel or at an angle of up to 45 deg to the collision direction in other systems mentioned previously. The formation of elongated grains was considered to be a result of plastic flow during explosive cladding.[5,6,7] There is no evidence of the existence of elongated grains in the present system, but randomly oriented twins are observed just below the bonding interface, as shown in Figure 5(a). The origin of this difference is not clear, but it may be related to the difference in the deformation mechanism between hexagonal close-packed and cubic metals. In other words, multiple twin systems can be operative in the former but not in the latter during deformation. The crystallographic characterization of these twins will be discussed in the companion article.[19]

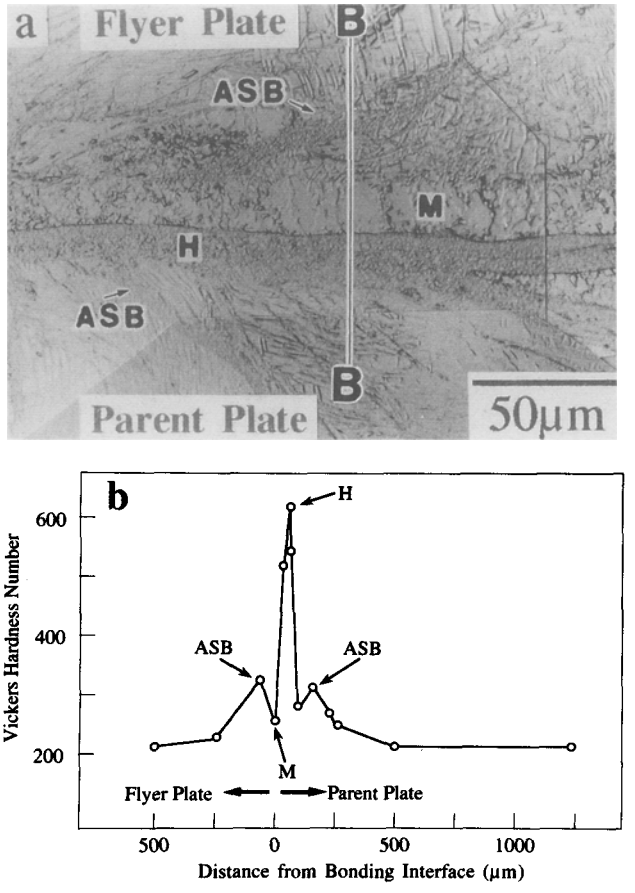

Fig. 8—(*a*) Optical micrograph around the bonding interface in system VI, where M, H, and ASB indicate melt layer, hardening zone, and adiabatic shear band, respectively. (*b*) Vickers microindentation hardness measured along line B in (a).

C. *Anomalously Hardened Zone of Bonding Interface in System VI*

Figures 8(a) and (b) show an optical micrograph of the bonding interface in system IV and corresponding hardness distribution along line B in (a), respectively. The average hardness values of melt zone (marked M) and adiabatic shear band (marked ASB) are about 260 and 300 VHN, respectively. The hardness of band structure with dark contrast between the melt layer and the parent plate, marked H, is extremely high, about 600 VHN, which is twice that of the martensitic phase in pure titanium.[23] One of the possible causes of this anomalous hardening is considered to be the contamination of interstitial impurity elements, such as oxygen.[24] Therefore, AES analysis was carried out in and around the hardening zone, as shown in Figure 9. A secondary electron image of the hardening zone is given in Figure 9(a). The AES spectra in Figures 9(b) and (c) are taken from positions B and C, respectively, in Figure 9(a). Argon is detected in both cases, since the specimens were spattered by argon ion for 2 hours before analysis. Carbon and oxygen were detected at a position C, which is the center of the hardening zone, while these two elements could not be detected at a position B, which is at a distance of 80 μm from C. Figure 9(d) shows a line profile of AES analysis along line D in Figure 9(a). It is obvious from these results that carbon and oxygen enriched the hardening zone. However, the anomalous hardening cannot be explained by only solid solution hardening of the carbon and oxygen, according to the previous investigation by Jafee *et al.*[24] Subsequently, TEM observations were performed on the hardening zone.

Figure 10(a) shows a bright-field image of the hardening zone, which consists of fine grains less than 200 nm in diameter. There was no evidence of the formation of carbide and oxide particles on a conventional TEM scale. Figure 10(b) shows a dark-field image for one of the fine grains in the hardening zone. There is considerable density of dislocation images in the grain interior. Some of those form a network structure. Figure 10(c) shows the electron diffraction pattern taken from microtwin C in Figure 10(a). The twinning plane of those has been determined to be $(01\bar{1}1)$. This is a dominant twinning system in deformation structure above 673 K[25] and an internal defect of the martensitic phase in pure titanium,[23] as mentioned previously. It is concluded that the hardening zone is a sort of work-hardening state, and its formation mechanism is different from that of the ASB,[9,11,12,19] in spite of similar morphology. Hence, a possible cause should be considered to be ω-phase formation at high pressure under a shock-loading condition.[26] This could not be identified by the present electron diffraction experiments, but this possibility cannot be neglected absolutely. Further detailed analysis will be required by using such precise techniques as neutron diffraction. Consequently, the origin of anomalous hardening may be ascribed to be the mutual effects of solid solution hardening due to interstitial elements, grain refinement, and work hardening of fine grains.

However, an essential question is not clear from the

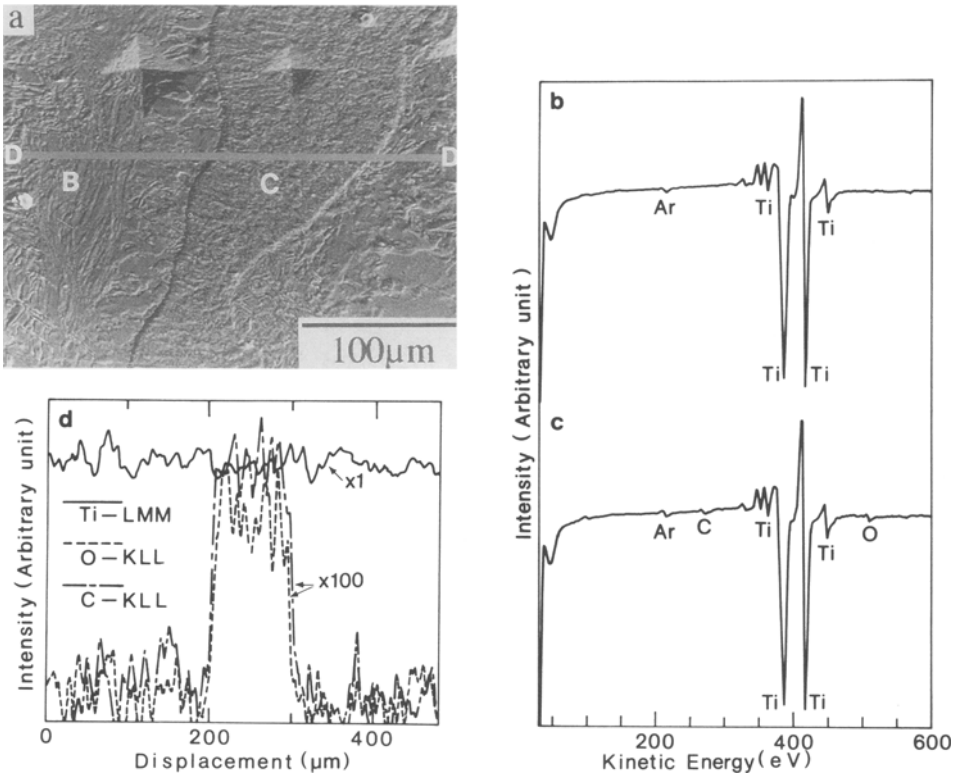

Fig. 9—(*a*) Secondary electron image of the hardening zone. (*b*) and (*c*) AES spectra obtained from points marked B and C in (a), respectively. (*d*) AES spectra profile for Ti, C, and O along line D in (a).

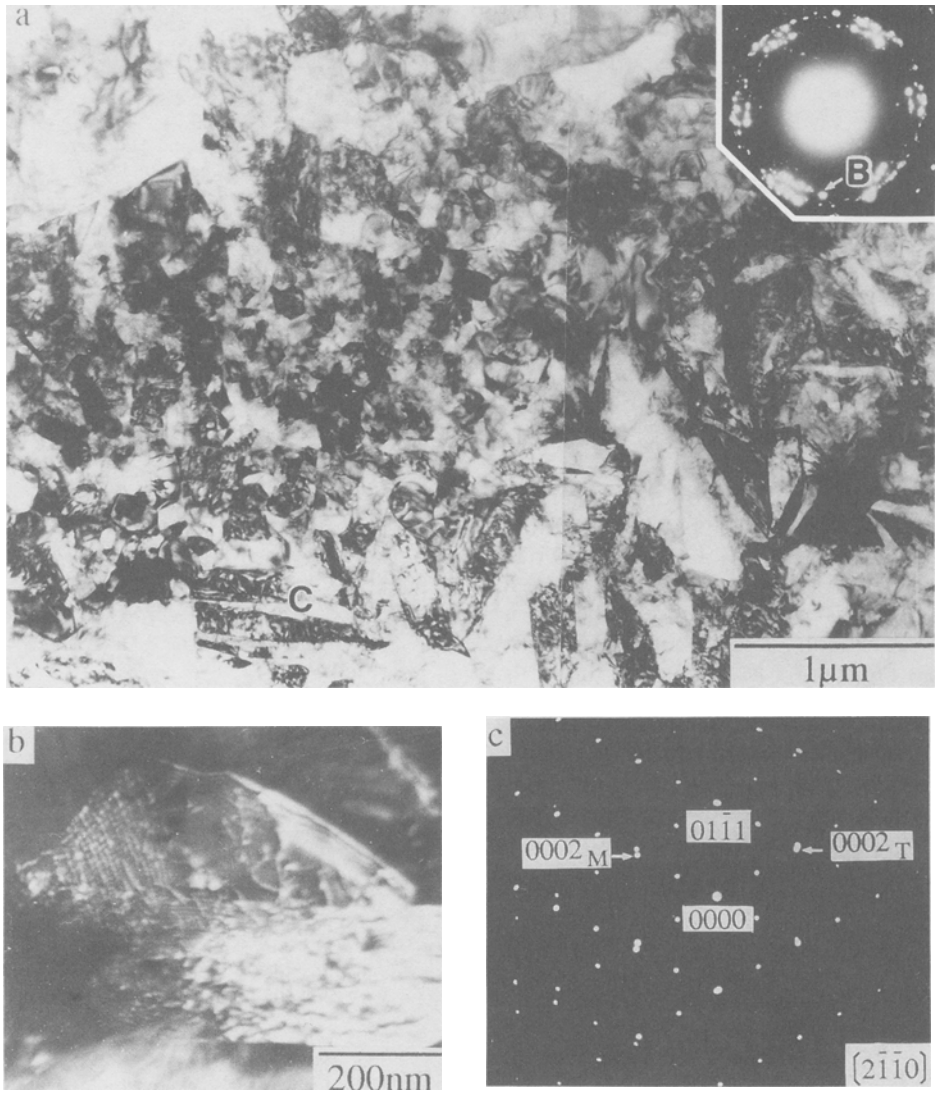

Fig. 10—Transmission electron micrographs of microcrystalline features observed within hardening zone at the bonding interface. (*a*) Bright-field image, (*b*) enlarged dark-field image taken by using a diffraction spot marked B in the SAD pattern of (a), and (*c*) corresponding electron diffraction pattern of microtwin C in (a) showing (01$\bar{1}$1) twinning.

previously mentioned results. That is the question of why the hardening zone was confined at the parent plate side in the bonding interface. This is considered as follows. The hardening zone consists of fine grains, as described earlier. These fine grains may be related to the metal jet, which consists of solid-state particles, including impurity elements derived from metal surfaces, and is formed at the apex of the collision. This is supported by the result of AES analysis, which shows the contamination of carbon and oxygen in the hardening zone. It is likely that the metal jet was locked between the melt layer and the parent plate. In other words, the contact of flyer and parent plates and the formation of metal jet occurred concurrently because of higher flyer plate speed in system VI. Then, the collision energy, which acts as the formation of wavy interface, is consumed by plastic deformation of the metal jet. This can explain the consistently formed planar interface in system VI. From a practical standpoint, such hardening zone may cause the degradation of bonding strength in explosively welded Ti clad materials and should be eliminated by controlling clad parameters.

IV. CONCLUSIONS

Microstructural modifications of the bonding interface in an explosively welded Ti/Ti clad material using the preset angle standoff configuration have been studied, and the following conclusions have been drawn.

1. Explosive welding was completed at flyer plate speed of more than 420 m/s. The formation of ASBs was observed in the clad materials welded at flyer plate speed of more than 820 m/s. The wavelength and amplitude of the wavy interface increased with increasing flyer plate speed up to 1060 m/s. The planar

interface was obtained at flyer plate speed of 1150 m/s.
2. The trace of melting was observed at the bonding interface within the present experimental conditions. That is, the melting layer was responsible for the bonding of explosively welded Ti/Ti clad materials.
3. An anomalous hardening zone formed at the bonding interface in the clad material welded at flyer plate speed of 1150 m/s. The origin of anomalous hardening has been ascribed to mutual effects of solid solution hardening due to interstitial elements and work hardening of fine grains, likely related to the plastic deformation of the metal jet.

ACKNOWLEDGMENTS

This work was partially supported by a Grant-in-Aid for Fundamental Scientific Research (Ippan-C, 1986) from the Ministry of Education of Japan. The authors would like to express their appreciation to Dr. T. Watanabe of Tohoku University for his critical reading of the manuscript and valuable comments. The authors also express their thanks to Professor M. Fujita and Mr. N. Tsukimata of the High Energy Rate Laboratory, Kumamoto University, for kind assistance in explosive experiments. The authors are also grateful to Mr. Y. Nagasawa of JEOL Ltd. for his skillful help on the AES analysis. The titanium plate and the explosives were kindly provided by the Nippon Steel Co., Ltd., and the Asahi Chemical Industry Co., Ltd., respectively.

REFERENCES

1. T. Kawanami: *J. Jpn. Soc. Technol. Plasticity*, 1991, vol. 32, pp. 1-12.
2. B. Crossland: *Explosive Welding of Metals and Its Application (Oxford Series on Advanced Manufacturing; 2)*, Oxford, United Kingdom, 1982, pp. 10-38.
3. S.H. Carpenter: in *Shock Waves and High-Strain-Rate Phenomena in Metals (Concepts and Applications)*, M.A. Meyers and L.E. Murr, eds., Plenum Press, New York, NY, 1981, pp. 941-59.
4. E. Ganin, Y. Komen, and B.Z. Weiss: *Acta Metall.*, 1986, vol. 34, pp. 147-58.
5. C.H. Oxford and P.E.J. Flewitt: *Metall. Trans. A*, 1977, vol. 8A, pp. 741-50.
6. J. Dor-Ram, B.Z. Weiss, and Y. Komen: *Acta Metall.*, 1979, vol. 27, pp. 1417-29.
7. M. Hammerschmidt and H. Kreye: in *Shock Waves and High-Strain-Rate Phenomena in Metals (Concepts and Applications)*, M.A. Meyers and L.E. Murr, eds., Plenum Press, New York, NY, 1981, pp. 961-73.
8. L.E. Murr: in *Shock Waves and High-Strain-Rate Phenomena in Metals (Concepts and Applications)*, M.A. Meyers and L.E. Murr, eds., Plenum Press, New York, NY, 1981, pp. 607-73.
9. R.L. Woodward: *Metall. Trans. A*, 1979, vol. 10A, pp. 569-73.
10. Y. Me-Bar and D. Shechtman: *Mater. Sci. Eng.*, 1989, vol. 58, pp. 181-88.
11. H.A. Grebe, H.-R. Pak, and M.A. Meyers: *Metall. Trans. A*, 1985, vol. 16A, pp. 761-75.
12. M.A. Meyers and H.-R. Pak: *Acta Metall.*, 1986, vol. 34, pp. 2493-99.
13. G.T. Gray III: *Acta Metall.*, 1988, vol. 36, pp. 1745-54.
14. J.C. Huang and G.T. Gray III: *Mater. Sci. Eng.*, 1988, vol. A103, pp. 241-55.
15. J.C. Huang and G.T. Gray III: *Scripta Metall.*, 1988, vol. 22, pp. 545-50.
16. P.S. Follansbee and G.T. Gray III: *Metall. Trans. A*, 1989, vol. 20A, pp. 863-74.
17. J.C. Huang and G.T. Gray III: *Metall. Trans. A*, 1989, vol. 20A, pp. 1061-75.
18. J.C. Huang and G.T. Gray III: *Acta Metall.*, 1989, vol. 37, pp. 3335-47.
19. M. Nishida, A. Chiba, S. Ando, K. Imamura, and H. Minato: *Metall. Trans. A.*, 1993, vol. 24A, pp. 743-50.
20. B. Crossland: *Explosive Welding of Metals and Its Application (Oxford Series on Advanced Manufacturing; 2)*, Oxford, United Kingdom, 1982.
21. H.K. Wylie, P.E.G. Williams, and B. Crossland: in *Proc. 3rd Int. Conf. of the Center for High Energy Rate Forming*, Denver Research Institute, Denver, CO, 1971, pp. 1.3.1-1.3.43.
22. J. Shudo, T. Sato, M. Nishida, and A. Chiba: in *Collected Abstracts of the Annual Fall Meeting of Japan Institute of Metals*, Japan Institute of Metals, Sendai, Sendai 980, Japan, 1990, p. 414.
23. Z. Nishiyama, M. Oka, and H. Nakagawa: *Trans. Jpn. Inst. Met.*, 1966, vol. 7, pp. 168-73.
24. R.I. Jafee, H.R. Ogden, and D.J. Maykuth: *Trans. AIME*, 1950, vol. 1888, pp. 1211-66.
25. N.E. Paton and W.A. Backofen: *Metall. Trans.*, 1970, vol. 1, pp. 2839-47.
26. G.T. Gray III: in *Shock Compression of Condensed Matter—1989*, S.C. Schmidt, J. N. Johnson, and L.W. Davison, eds., Elsevier Science Publishers B.V., Amsterdam, pp. 407-17.